



# Kinetic and equilibrium studies for U(VI) and Cd(II) sorption from commercial phosphoric acid using C100H resin

Amir A. Elzoghby<sup>1</sup>

Received: 28 March 2021 / Accepted: 7 June 2021 / Published online: 16 June 2021

© This is a U.S. government work and not under copyright protection in the U.S.; foreign copyright protection may apply 2021

## Abstract

The present work aims to uranium and cadmium ions sorption from commercial di-hydrate phosphoric acid using commercial cation exchange resin, C100H. The influence of main factors such as shaking time, sorbent dose, and phosphoric acid molarity have been investigated to figure out the sorption characteristics of C100H resin. The displayed results declare the applied cation exchange resin have high tendency for U(VI) and Cd(II) sorption from crude phosphoric acid whereas about 95.8% and 82.5% of uranium and cadmium ions respectively were removed successfully from phosphoric acid. The kinetic and isotherm of the sorption process show that U(VI) and Cd(II) sorption obey the pseudo-second order kinetic model and Langmuir isotherm model. The sorption capacity of C100H resin for U(VI) and Cd(II) ions were 14.6 and 3.3 mg/g. The desorption of U(VI) and Cd(II) from loaded resin were performed and the resin exhibit high stability for 6 sorption/desorption cycles.

**Keywords** Kinetic · Uranium · Cadmium · Sorption · Phosphoric acid · Commercial resin

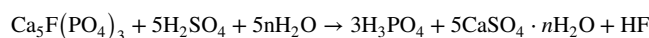
## Introduction

Phosphate fertilizers are essential for plant growth and productivity. Therefore, phosphate fertilizers play an important role in the food security system [1, 2]. Hence, as the world population increases, the food demand increases which in turn increase the global phosphate fertilizers demand [3]. The United Nations reported that worldwide, the food production is expected to increase by 70% by 2050 as a result in the world population increases over 9 billion, which means that the world demand of phosphate fertilizers is in turn increases [3, 4].

Phosphate rock (which is a sedimentary or igneous rocks mined from clay deposits) is the main sources of phosphate fertilizers [5]. Phosphate rock is mainly mined and processed to form phosphoric acid as well as elemental phosphorus. Processed phosphate is used in several applications, for example: fertilizers, animal feed, detergent, food, and beverages [5, 6].

Phosphate rocks naturally contain minor concentrations of uranium as well as toxic elements such as cadmium. The level of potentially toxic metals in the phosphate rock depends on the type and the origin of the phosphate rock whereas; sedimentary phosphate deposits possess much higher concentrations of potentially hazardous elements (uranium and cadmium) than igneous rock phosphate deposits [5–8]. Cadmium concentration in phosphate rock varied from 3–150 mg/kg with average concentration of 18 mg/kg, while uranium concentration in phosphate rock is ranging from 20 to 500 mg/kg with average concentration of 100 mg/kg [7–9]. These elements are classified as carcinogenic, non-biodegradability, and bio-accumulation [10]. The long term application of phosphate fertilizers increases the level of these hazards in the environment and subsequently to the human body via the food chain [5–7].

Mainly, phosphoric acid is produced from phosphate rock using the sulfuric acid in the so called wet process based on the following equation:



During the wet production process, most of uranium and cadmium is transferred into the phosphoric acid and in turn in the phosphate fertilizers [5–7]. Accordingly, the removal of these hazardous will improve the quality of the

✉ Amir A. Elzoghby  
amirelzoghby33@gmail.com

<sup>1</sup> Department of Chemistry, Nuclear Materials Authority, P.O. Box 530, ElMaadi, Cairo, Egypt

phosphoric acid, and prevent their spread on agricultural land. In addition, uranium recovery from phosphoric acid could supply a significant part of the uranium requirement worldwide [8].

Uranium as well as cadmium recovery from phosphoric acid has been performed using different approaches, for instance: co-precipitation, solvent extraction, membrane-based separation, and adsorption on different surfaces [11–15]. Despite of solvent extraction is the only proven process for the recovery of heavy metals and uranium from phosphoric acid; however, it suffers from several disadvantages such as: leads to the contamination of phosphoric acid with organic solvents, large consumption of combustible carriers, generating large amounts of solvent waste, and crud formation [16–18].

Solid–liquid extraction of toxic and radioactive elements from aqueous solutions has proven to be more advantageous, for example: strong flexibility and kinetic properties, high sorption power, its low rate of physical deterioration, and the absolute insolubility of the applied solid in the aqueous process [17–20]. Numerous solid materials have been investigated for the purification of phosphoric acid, for example: DEHPA – TOPO solvent immobilized in calcium alginate [21], white silica sand [22], activated bentonite [23], Cyanex 923- DEHPA encapsulating in poly(ether sulfone)-based composite [24], and solvent impregnated charcoal [25]. However, the above materials are to somewhat cumbersome in reuse and recovery [19, 20].

Ion-exchange and chelating resins are commonly used for the hydrometallurgical recovery of radioactive and toxic elements from aqueous solutions whereas they are characterized by the ability to reuse for several cycles of sorption/desorption, and acid and heat resistances [17–21]. Commercial resins were applied for the recovery of radioactive as well as toxic elements from phosphoric acid, such as: the recovery of REEs from phosphoric acid using Lewatit VP OC 1026, Lewatit TP-260, Amberlite IRC-747, Purolite S940, and Tulsion CH-93 have been investigated for REEs recovery from phosphoric acid [19, 20]. Marathon C cationic exchange resin has applied for the recovery of U(VI), Cd(II), Mn(II), Zn(II) and Cu(II) from phosphoric acid [26]. Duolite ES467 (amino-phosphonic resin), and Duolite C464 (hydroxy-phosphonic resin), MTC1600H (sulfonic cationic exchanger), MTS9500 (aminophosphonic-chelating resin), and MTS9570 (phosphonic/sulfonic chelating resins) have been applied to recover cadmium and uranium ions from phosphoric acid [17, 18]. Nevertheless, these trails attempts have never been applied industrially [19, 20, 27].

In this contribution, commercial sulfonic cationic exchanger resin (C100H) has been applied for the sorption of uranium and cadmium ions from industrial phosphoric acid as an effective alternative method to the conventional solvent extraction method. The main variables influencing

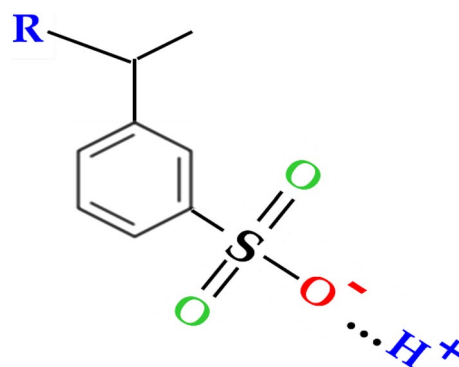


Fig. 1 The functional group of C100H resin

Table 1 Main physical and chemical properties of C100H resin

Polymer structure	Gel polystyrene crosslinked with divinylbenzene
Appearance	Spherical beads
Functional group	Sulfonic acid
Ionic form as shipped	H <sup>+</sup>
Total capacity (min.)	2.0 eq/L (H <sup>+</sup> form)
Moisture retention capacity	51–55% (H <sup>+</sup> form)
Specific gravity	1.2 (H <sup>+</sup> form)
Particle size range	300–1200 μm
Temperature limit	120 °C

the sorption efficiency such as: sorbent dose, shaking time, phosphoric acid molarity, and the sorption isotherms, and kinetics were studied. Desorption and sorbent recycle have been performed.

## Materials and methods

### Materials

Purolite strong cation exchange resin (C100H) has been supplied from Purolite Co. Ltd. (Qianyuan, China). The functional group of the resin was shown in Fig. 1, and the main physical and chemical characteristics of the applied resin were presented in Table 1. The resins were washed with deionized water and then conditioned in an acid solution of composition and pH matching the experimental conditions. Commercial di-hydrate phosphoric acid sample utilized in this work were purchased from Abu Zaabal Company for Fertilizer and Chemical Materials (AZFC), and used without any purification processes. The chemical properties of the crude phosphoric acid sample have been displayed in Table 2 as analyzed in Nuclear Materials Authority.

## Procedures

The experimental work was performed by shaking a proper weight of resin with 4.0 M phosphoric acid (containing 40 and 16 mg/L of uranium and cadmium ions concentration respectively) in 10 mL in polyethylene tubes at ambient temperature. The impact of different variables on U(VI) and Cd(II) removal process such as shaking time (2–600 min), sorbent dose (0.5–5 g/L), phosphoric acid molarity (2–6 M) were investigated using batch wise route. The experiments were carried out in triplicate and ~5% relative error has been accepted. After the reaction proper time, a subsequent filtration is performed to separate the solid and liquid phases. Uranium concentration in the phosphoric acid has been measured using Shimadzu UV–Visible recording spectrophotometer type UV-60A by applying Arsenazo-III spectrophotometer method at 650 nm [28] and titrimetric method [29] while cadmium concentration has been measured using Atomic Absorption Spectrometer GBC 932 AA (UK).

The quantity of adsorbed ions ( $q_t$ ) has been evaluated from the difference between the metal ion concentrations before ( $C_o$ , mg/L) and after ( $C_e$ , mg/L) the sorption process based on the following equation.

$$q_e = (C_o - C_e) \times \frac{V}{m} \quad (1)$$

where  $q_t$  (mg/g) is the amount of ion adsorbed at time  $t$ ,  $V$  (L) is the phosphoric acid solution volume and  $m$  (g) is the resin mass. The distribution coefficient ( $K_d$ ) and the sorption efficiency percent could be described according to Eqs. 2 and 3 respectively:

$$K_d = \frac{(C_o - C_e)}{C_o} \times \frac{V}{m} \quad (2)$$

**Table 2** Chemical properties of commercial phosphoric acid

Element	Phosphoric acid
Composition Wt %	
P <sub>2</sub> O <sub>5</sub>	≈ 24.5
SO <sub>4</sub>	2.1
F	0.7
Fe <sub>2</sub> O <sub>3</sub>	0.81
Trace elements (ppm)	
Mn	536
Zn	190
Cd	16
U	40

$$E\% = 100 \times \frac{(1 - C_e)}{C_o} \quad (3)$$

## Modeling of sorption process

### Adsorption isotherm models

The adsorption isotherm has been investigated for improving the U(VI) and Cd(II) sorption system as well as performs the plant design. Accordingly, U(VI) and Cd(II) sorption isotherm has been investigated using the following isotherm models, Langmuir, Freundlich, and Temkin Isotherm equations [Eqs. (4), (5), and (6), respectively] [30, 31].

$$\frac{C_e}{q_e} = \frac{1}{bQ_o} + \frac{C_e}{Q_o} \quad (4)$$

$$\log q_e = \log k_f + \frac{1}{n} \log C_e \quad (5)$$

$$\ln q_e = \ln q_m + \beta \varepsilon^2 \quad (6)$$

where  $C_e$  is concentration of adsorbate at equilibrium (mg/L),  $q_e$  is amount of the adsorbate at equilibrium (mg/g),  $b$  is the Langmuir constant related to affinity of adsorbent and the enthalpy of sorption (L/mg),  $q_m$  is maximum monolayer coverage capacities (mg/g),  $k_f$  is adsorption capacity (L/mg); ( $n$ ) is adsorption intensity;  $T$  is the temperature (K);  $R$  is the ideal gas constant (8.314 J/mol K),  $b_T$  is Temkin constant that refers to the adsorption heat, and  $K_T$  (L/min) is the equilibrium binding constant.

### Adsorption kinetic models

The adsorption kinetic is important parameter for predicting the adsorption rate of reaction as well as understanding the adsorption mechanism. In this regards, U(VI) and Cd(II) sorption kinetics have been investigated using The Lagergren pseudo first-order model, the pseudo-second order model, and Weber and Morris model, [Eqs. (7), (8), and (9) respectively] [31, 32].

$$\log (q_e - q_t) = \log q_e - \frac{k_1}{2.303} t \quad (7)$$

$$\frac{t}{q_t} = \frac{1}{k_2 q_e^2} + \frac{1}{q_e} t \quad (8)$$

$$q_t = K_{id} t^{0.5} + C \quad (9)$$

where  $q_t$  is the sorption capacity at time  $t$  (mg/g),  $K_1$  is the rate constant of the pseudo first-order sorption ( $\text{min}^{-1}$ ),  $t$

is time (min),  $K_2$  is the rate constant of the pseudo second order kinetics (g/mg min),  $K_{id}$  is intraparticle diffusion rate constant (mg/g min<sup>1/2</sup>),  $C$  is the initial adsorption (mg/g).

## Results and discussion

The following section represents the results obtained from the application of C100H cation exchange resin for U(VI) and Cd(II) sorption from di-hydrate phosphoric acid. The impact of resin dose, shaking time as well as the phosphoric acid molarity on the sorption efficiency has been investigated. The sorption isotherm and kinetics were performed. Desorption process has been achieved using several aqueous solutions.

### Influence of sorbent dose

The effect of C100H dose on U(VI) and Cd(II) sorption from 4.0 M phosphoric acid has been investigated for sorbent dose ranging from 0.5 to 5.0 g/L while the other parameters were fixed at 24 h reaction time and room temperature. The obtained data have been displayed in Fig. 2 as a relation between the sorption efficiency and resin dose. The revealed results declares that, as the resin dose increases from 0.5 to 6.0 g/L the sorption efficiency of increases strongly from 17.8 to 97.3% for U(VI) and from 10.0 to 88.8% for Cd(II) respectively. This behavior could be attributed to the presence of more resin active sites [18]. Further increase in sorbent dose has slightly positive impact on the uranium and cadmium ions sorption efficiency. Therefore, sorbent dose of 5.0 g/L has been selected for the other experiments.

Despite of the uranium and cadmium ions sorption efficiency increases with the resin dose increases; however, it is clear that the sorption quantity of the metal ions decreases with the increase of sorbent dose as displayed in Fig. 2. Numerically, as the resin dose increases from 0.5 to 6.0 g/L, the sorption quantity decreases from 14.2 to 6.5 mg/g for U(VI) and from 3.2 to 2.4 mg/g for Cd(II). This behavior could be due to the available reaction sites on the resins were not free available for reacting with uranium and cadmium ions, and the low concentration of U(VI) and Cd(II) could not meet the adsorption capacities of adsorbents, and thereby decreased the  $q_e$  [18, 23].

### Sorption isotherm

The isotherm of the application of C100H resin for U(VI), and Cd(II) ions sorption from industrial phosphoric acid has been performed using the linear equations of Langmuir, Freundlich, and Temkin models. The equilibrium isotherm analysis is explored in Figs. 3, 4 and 5 respectively. The values of the isotherm parameters were obtained and displayed in Table 3. The Fitting of the isotherm model was tested using the values of the correlation coefficient.

The  $\log q_e$  as a function of  $\log C_e$  (Freundlich model plot) for U(VI) and Cd(II) sorption has been displayed in Fig. 3. From the figure, it is clear that the relation between  $\log q_e$  and  $C_e$  gives straight lines with  $R^2$  equals (0.96). The heterogeneity factor ( $n$ ) for both uranium and cadmium is higher than 1.0 (Table 3) which indicates that the metal ions sorption using C100H is favorable [18, 33]. Uranium adsorption using C100H has higher  $k_f$  value than cadmium, which

**Fig. 2** Effect of sorbent dose on U(VI) and Cd(II) sorption efficiency, % (phosphoric acid concentration 4.0 M; temperature 298 K; shaking time 24 h.)

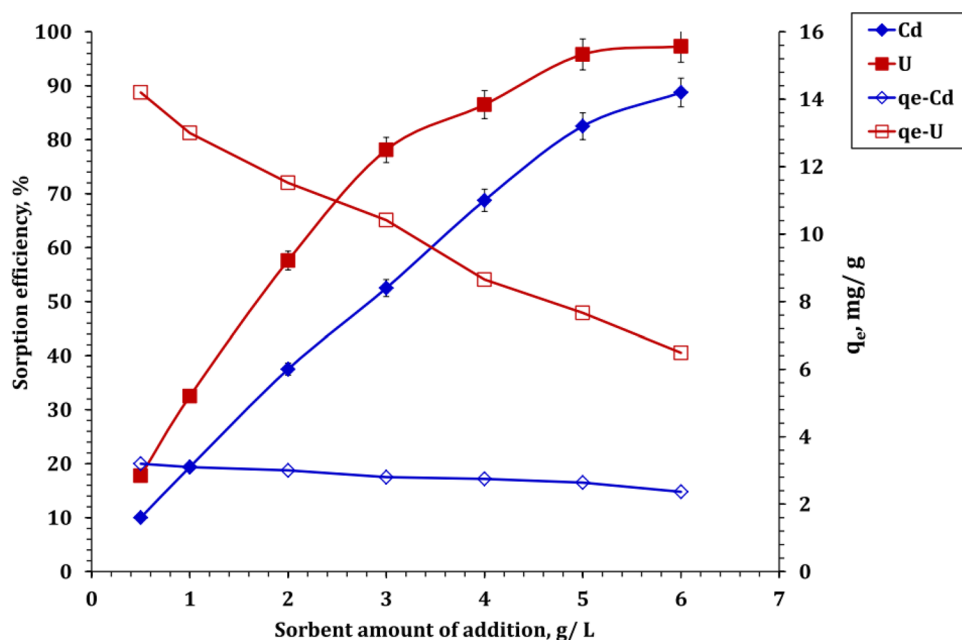


**Fig. 3** Freundlich model plot for U(VI) and Cd(II) sorption from commercial phosphoric acid

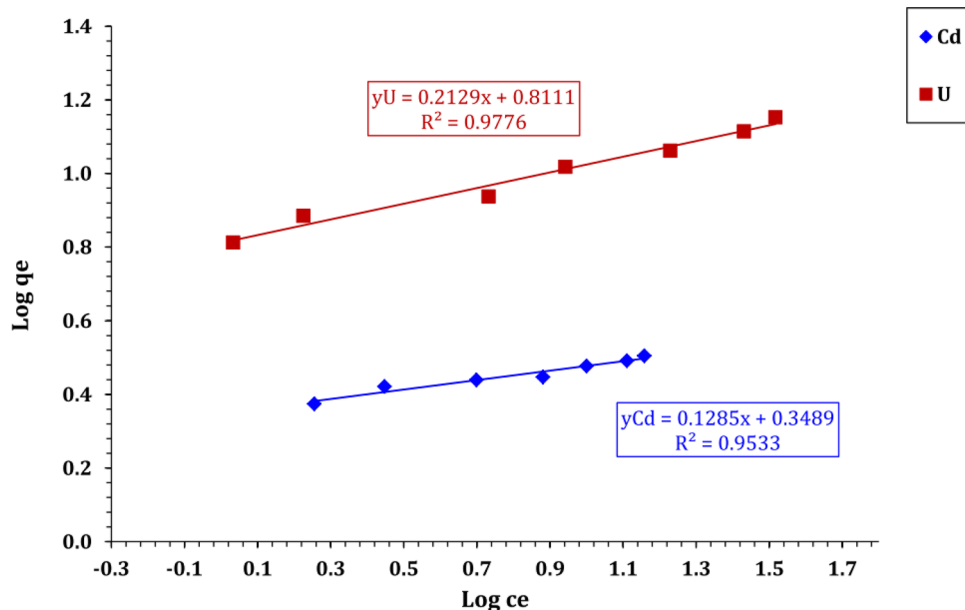
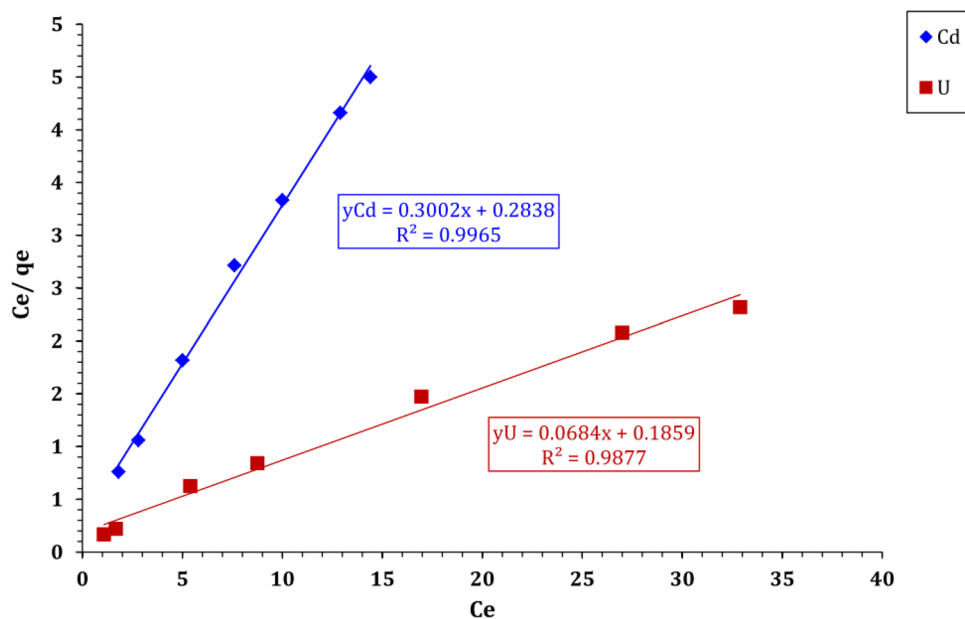


**Fig. 4** Langmuir model plot for U(VI) and Cd(II) sorption from commercial phosphoric acid



indicates that the utilized resin has higher tendency for uranium ions than cadmium ions as shown in Table 3 [34].

Langmuir isotherm model describe the relation between  $C_e/q_e$  as a function of  $C_e$  (Fig. 4). According to Fig. 4, it is clear that Langmuir model exhibit linear relationship for both U(VI) and Cd(II) sorption from crude phosphoric acid with perfect correlation coefficient ( $R^2 = 99$ ). This means that the sorption process could be described successfully using Langmuir model, which declare that the sorption of uranium and cadmium is homogenous process, and the applied commercial resin has equivalent and identical active sites. Furthermore, the sorption of U(VI) and Cd(II) is monolayer and it occurs at exact number of resin active sites. This result is matches with

the results reported with other authors [18, 35]. The displayed data in Table 3 show that C100H sorption capacity is about 14.6 and 3.3 mg/g for U(VI) and Cd(II) respectively, which confirmed that the applied resin has higher tendency regards uranium ions than cadmium ions.

The natural of uranium and cadmium adsorption process whether the sorption is favorable or unfavorable could be declared by the dimensionless constant separation factor ( $R_L$ ) based on the following equation [35, 36]:

$$R_L = 1/(1 + k_L C_o) \tag{10}$$

**Fig. 5** Temkin model plot for U(VI) and Cd(II) sorption from commercial phosphoric acid

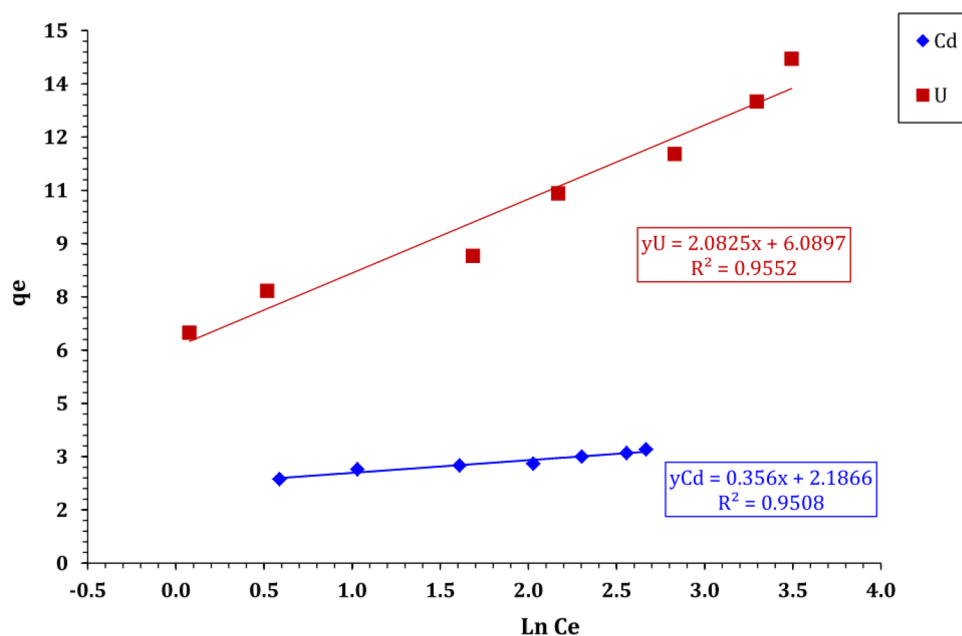


**Table 3** Isotherm parameters of Freundlich, Langmuir, Temkin isotherm models

	Cd	U
Freundlich isotherm model		
$n$	7.8	4.7
$K_f$ (mg/g)	2.2	6.5
$R^2$	0.95	0.97
Langmuir isotherm model		
$Q_m$ (mg/g)	3.3	14.6
$b$ (L/mg)	1.06	0.37
$R_L$	0.02	0.06
$R^2$	0.99	0.98
Temkin isotherm model		
$b$ (J/mol)	6959.4	1189.7
$B$	0.4	2.1
$KT$ (L/g)	465.0	18.6
$R^2$	0.95	0.95

The sorption is favorable if  $0 < R_L < 1$ , however it is unfavorable if  $R_L > 1$ , and the sorption is irreversible if  $R_L = 0$  [35, 36]. According to the results obtained in Table 3, it is indicated that uranium and cadmium ions using C100H is favorable where  $R_L$  equals 0.02 and 0.06 for Cd(II) and U(VI) respectively.

Temkin isotherm model links the heat of adsorption to the adsorbent surface [36]. The plot of Temkin isotherm model (Fig. 5) explores a linear relationship with correlation coefficient equal 0.95 for both metal ions sorption. The Temkin constant ( $b_T$ ) is 6.9 and 1.1 kJ/mol for Cd(II) and U(VI) ions (Table 3) which indicated that uranium

**Table 4** The experimental capacity of C100H resins compared with the sorption capacity of other sorbents for Cd(II) and U(VI) recovery from phosphoric acid

Sorbent	$q_m$ (mg/g)		References
	Cd(II)	U(VI)	
C100H resin	3.3	14.6	This work
Abu Zeneima white sand	0.14	0.87	[37]
White silica sand	n.r	0.14	[22]
0.05 M Triphenylphosphine sulphide impregnated charcoal	2.88	n.r	[25]
0.1 M Triphenylphosphine sulphide impregnated charcoal	4.18	n.r	[25]
Amberlite XAD-7-Cyanex-301	11.51	n.r	[38]
Amberlite XAD-2-Cyanex-301	1.56	n.r	[38]
Kaolinite	n.r	0.65	[23]
Metakaolinite	n.r	1.02	[23]
D <sub>2</sub> EHPA-impregnated charcoal	n.r	0.47	[15]
MARATHON C resin	7.29	14.7	[26]
MTC1600H resin	n.r	7.8	[18]
MTS9500 resin	n.r	10.6	[18]
MTS9570 resin	n.r	12	[18]

n.r. nor reported

and cadmium sorption using C100H commercial resin is a physisorption process [36].

The comparison between the maximum sorption capacity of C100H resin with other sorbents, available from literature, for uranium and cadmium sorption from phosphoric acid has been performed and displayed in Table 4. From the table, it is clear that C100H perform good

sorption capacity which indicates that C100H proven performance in established hydrometallurgy applications.

### Effect of shaking time

Several experiments were conducted to investigate the influence of reaction time in the range of 5–600 min on Cd(II) and U(VI) sorption from commercial phosphoric acid using C100H resin. The other parameters have been fixed at sorbent dose of 5.0 g/L resin, phosphoric acid concentration of 4.0 M and room temperature. The sorption efficiency has been explored as a function of the shaking time in Fig. 6. The collected data reveal that cadmium and uranium sorption process display fast sorption performance up to 60 min (the sorption percent were about 77.5%, and 93.8% for Cd(II) and U(VI) respectively). Further increase in reaction time is characterized by slight increase in the sorption efficiency. This means that the sorption of Cd(II) and U(VI) shows two stage sorption behavior; (1) fast up to equilibrium (60 min) due to the existence of free active groups on the resin surface, and (2) slow after equilibrium time due to the diffusion of the ions to interact with the inside active groups [39, 40]. Figure 6 explore that as the reaction time increases from 5 to 600 min, the sorption capacity of U(VI) and Cd(II) increases from 0.8 to 2.8 mg/g and from 2.4 to 7.9 mg/g respectively.

### Sorption kinetics

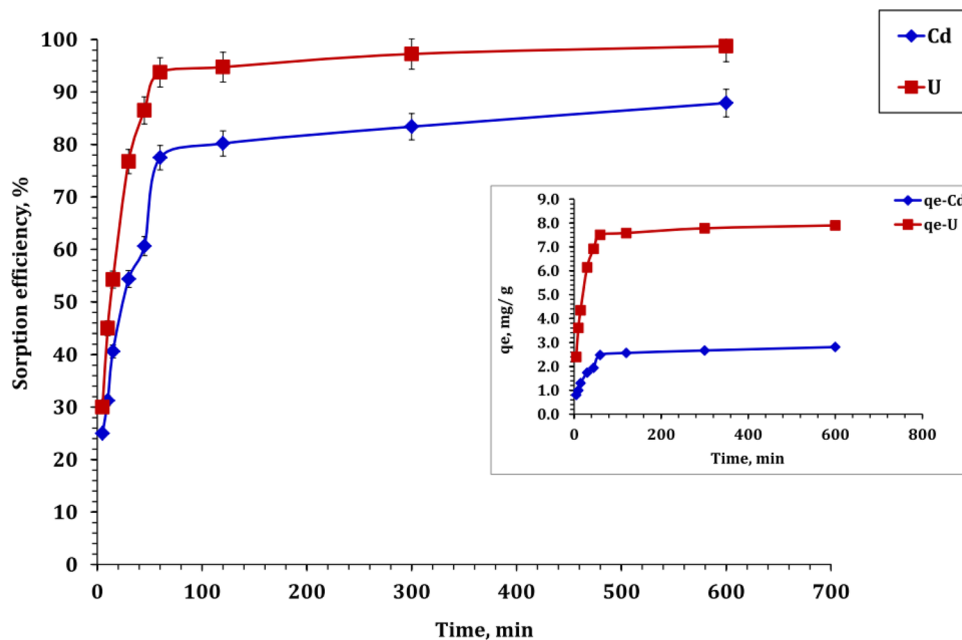
The kinetics of the sorption process is important to analyze the sorption rate of reaction as well as predicting the sorption mechanism. Accordingly, Lagergreen kinetic model,

pseudo-second order model, and Morris–Weber model have been applied to figure out the kinetics and mechanism of uranium and cadmium sorption from commercial dihydrate phosphoric acid using C100H resin. Figures 7, 8 and 9 represent the plots of Lagergreen, pseudo-second order, and Morris–Weber models respectively, while Table 5 display the obtained kinetic parameters. The fitting of the kinetic model has been declared based on the agreement between the experimental profiles and the fitted curve, as well as the obtained  $R^2$  coefficient.

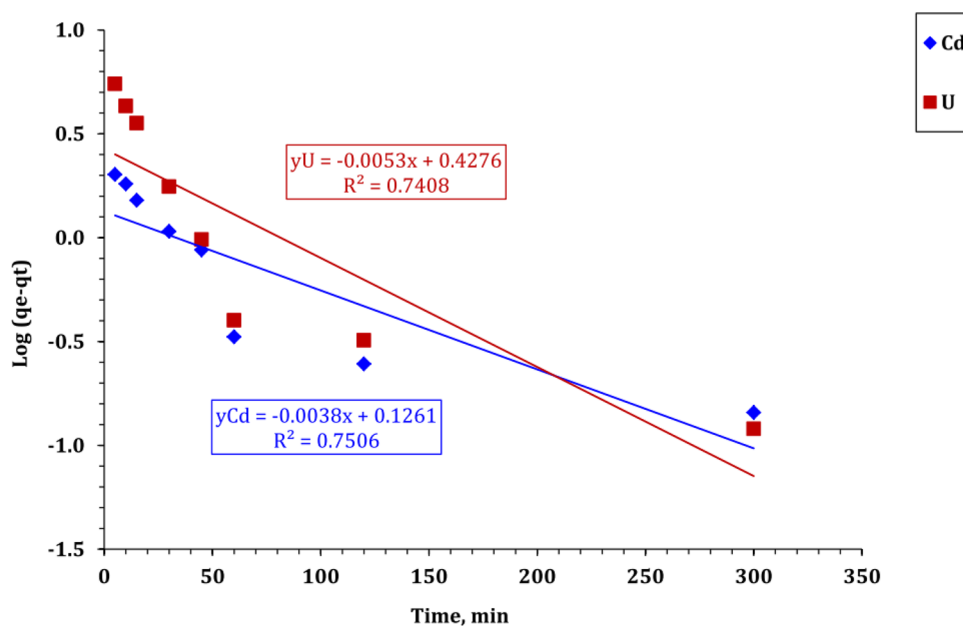
According to the data explored in Table 5, it is obvious that the relation between  $t/q_t$  and time display straight lines with  $R^2$  equals 0.99, and the value of sorption capacity calculated ( $q_{ecal}$ ) is close to the experimental sorption capacity ( $q_{exp}$ ) for both metal ions which reveals that the pseudo second order reaction model describe well the sorption of U(VI) and Cd(II) using C100H resin. This means that the sorption of U(VI) and Cd(II) is chemisorption process [31, 32]. This results in consistent with other previous reports [18, 26]. The applied resin exhibits higher sorption capacity at equilibrium for uranium (8.0 mg/g) than cadmium (2.9 mg/g). The half-equilibrium time,  $t_{1/2}$  (h), and initial adsorption rate,  $h$  (mol/g h) were evaluated from equations  $t_{1/2} = 1/(k_2 q_e)$  and  $h = k_2 q_e^2$  [32] and displayed in Table 5. The obtained data obvious that U(VI) sorption exhibit the lowest half equilibrium time (9.4) and the highest initial adsorption rate (0.85). On the other hand, Cd(II) sorption exhibit the highest half equilibrium time (17.2) and the lowest initial adsorption rate (0.17). These results indicate that C100H resin possess higher sorption tendency towards to U(VI) than Cd(II).

Figure 9 shows the variation of sorption capacity,  $q_t$ , as a function of time. From the figure it is clear that uranium

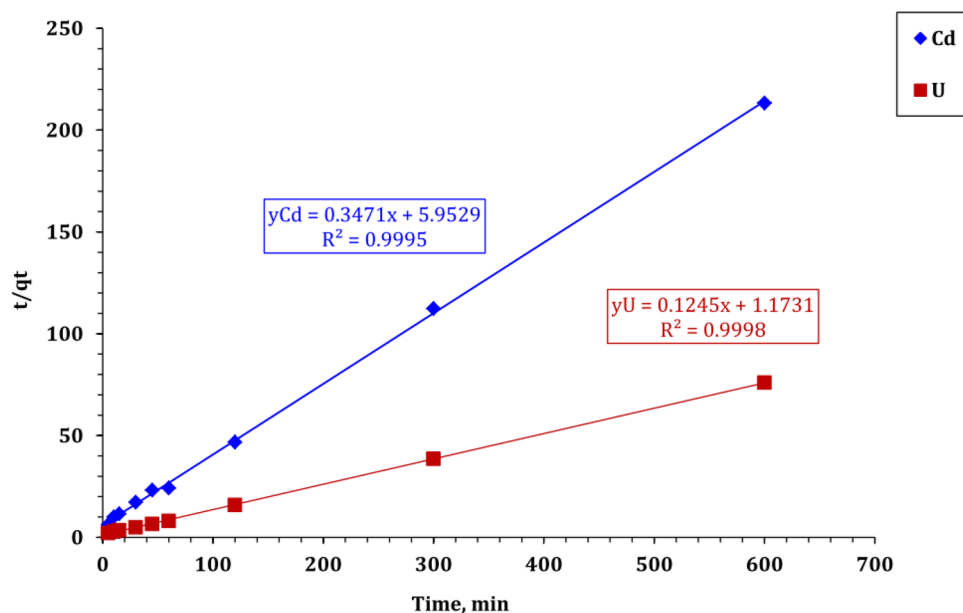
**Fig. 6** Effect of shaken time on Cd(II) and U(VI) sorption efficiency, % (4.0 M phosphoric acid molarity; 5.0 g sorbent/L; temperature 298 K)



**Fig. 7** Lagergreen plot for Cd(II) and U(VI) sorption from phosphoric acid



**Fig. 8** Pseudo second-order plot for Cd(II) and U(VI) sorption from phosphoric acid



and cadmium sorption process display multi-linear relationship which means that the intraparticle diffusion of cadmium and uranium species through the polymer bead was not the only mechanism of the sorption process [41]. The obtained data in Table 5 declare that the first stage has fast sorption rate and low diffusion resistance for both U(VI) and Cd(II) ions which indicate that the sorption occurs at the sorbent surface. On contrary, the second stage explores slow sorption rate and high diffusion resistance which indicate that the Intra-particle diffusion occurs [41, 42].

The difference between the sorption capacity (binding strength) of the resin towards the uranium and cadmium

metal ions could be explained based on the Pearson Hard and Soft Acids and Bases (HSAB) theory, which classified the ligands of the functional groups in resins as bases (i.e., electron donors), and the metal ions as acids (i.e., electron acceptors) [18, 31, 32]. In regards to the theory, strong bases will preferentially react with strong acid and reciprocal: weak bases with weak acids. Based on HSAB theory, the sulfonic group is strong base, and uranium is considered as strong acid, while cadmium is considered as weak acid. This means that C100H resin (with sulfonic



**Fig. 9** Morris–Weber illustration for Cd(II) and U(VI) sorption from phosphoric acid

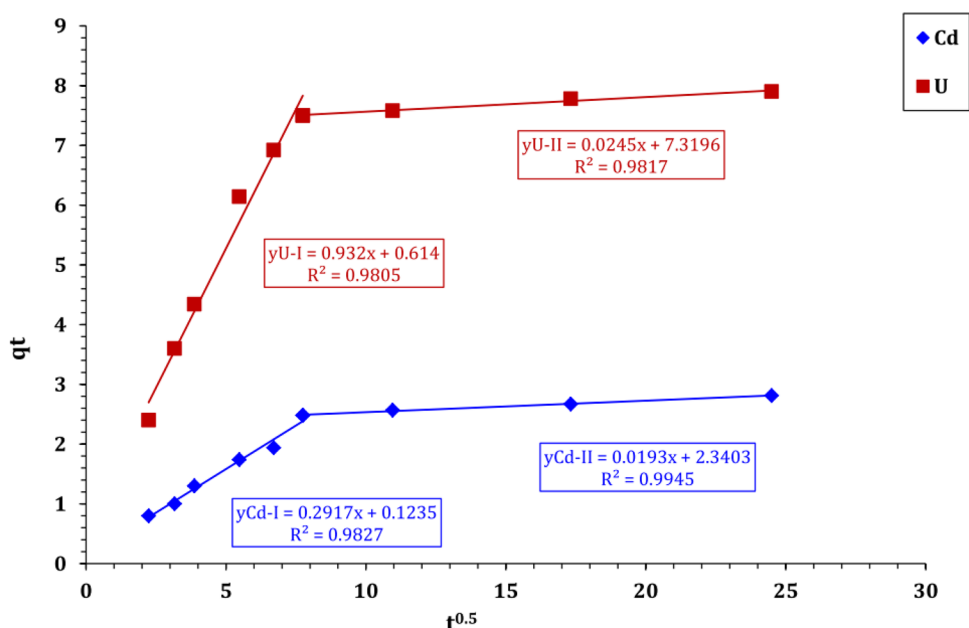


**Table 5** The calculated parameters of the pseudo first-order, pseudo second-order and Morris–Weber kinetic models

	Cd	U
<b>Lagergreen pseudo first-order</b>		
$K_1$ (min <sup>-1</sup> )	0.009	0.012
$q_{ecal}$ (mg/g)	1.3	2.7
$q_{eexp}$ (mg/g)	2.8	7.8
$R^2$	0.75	0.74
<b>Pseudo second-order</b>		
$K_2$ (min <sup>-1</sup> )	0.020	0.013
$q_{ecal}$ (mg/g)	2.9	8.0
$q_{eexp}$ (mg/g)	2.8	7.8
$h$ (mol/g h)	0.17	0.85
$t_{1/2}$ (h)	17.2	9.4
$R^2$	0.99	0.99
<b>Weber and Morris model</b>		
<b>Stage I</b>		
$K_i$ (mg/g min <sup>1/2</sup> )	0.29	0.02
$C$	0.1	2.3
$R^2$	0.98	0.99
<b>Stage II</b>		
$K_i$ (mg/g min <sup>1/2</sup> )	0.93	0.02
$C$	0.6	7.3
$R^2$	0.98	0.98

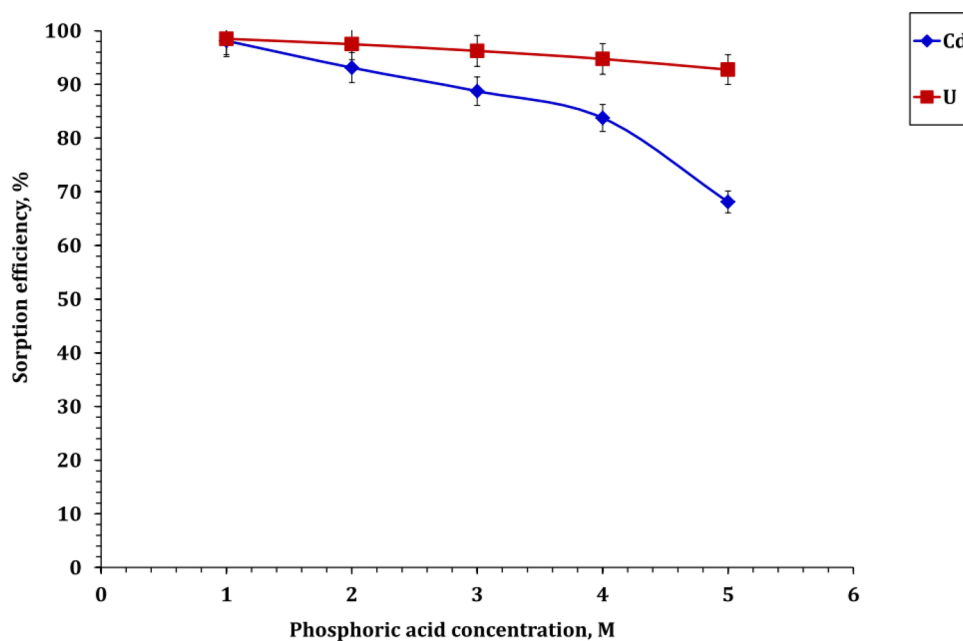
function group) will possess higher tendency towards uranium than cadmium. This tendency is agree with the obtained experimental results.

**Effect of phosphoric acid concentration**

Figure 10 explores the impact of phosphoric acid concentration ranging from 1.0 to 5.0 M on uranium and cadmium ions sorption percent using C100H cationic exchanger resin. The experimental conditions were fixed at 5.0 g/L resin dose, room temperature and 60.0 min shaking time. The displayed results indicated that uranium and cadmium sorption efficiency is negatively influenced with the variation of phosphoric acid molarity from 1.0 to 5.0 M. In details, Cd(II) and U(VI) sorption percent reduced from 98.1 to 68.1% for Cd(II) ions, from about 98.5 to 92.8% for U(VI) ions by varying phosphoric acid molarity from 1.0 to 5.0 M. This behavior suggests that Cd(II) and U(VI) sorption mechanism obey to ion exchange type mechanism at low phosphoric acid concentration [26, 43], while as the phosphoric acid molarity increases (pH decreases) the sorption mechanism is changed [43]. This performance could be due to the increase of phosphoric acid bulk density and in turn the increase of acid molecules accumulation over the sorbent surface which affect negatively on the Cd(II) and U(VI) ions diffusion to the sorbent surface [44]. Furthermore, the increase of acid molarity decreases the resin’s mobile ions and therefore reduces Cd(II) and U(VI) ions sorption percent. This behavior is in good agreement with the reported literature [18, 23, 27, 44].

The variation of phosphoric acid molarity influence on Cd(II) and U(VI) metal ions sorption efficiency could be due to the various speciation of Cd(II) and U(VI) ions in the phosphoric acid. To the author knowledge, U(VI) and Cd(II) ions exist predominantly in phosphoric acid molarity higher than 2.0 M as the following species  $UO_2(H_2PO_4)$

**Fig. 10** Influence of phosphoric acid molarity on Cd(II) and U(VI) ions removal percent, % (room temperature; shaking time 24 h; sorbent dose 3 g/L; 100 rpm)



$\text{H}_3\text{PO}_4^+$ , and  $\text{Cd}^{2+}$  [18, 23, 26]. This indicated that the interaction between the applied C100H resin and U(VI) and Cd(II) ions will involve the exchange of two  $\text{H}^+$  ions in case of cadmium ions, and only one  $\text{H}^+$  in case of uranium ion. The variation of  $\text{Log } K_d$  as a function of  $\text{Log}$  acid molarity is explored in Fig. 11. The figure declares a linear relationship for both metal ions with slope close to 1.0 in case of uranium ions and 2.0 in case of cadmium ions which in agreement with the obtained metal species in literature.

### Desorption investigation

The metal desorption is an important process for recycling the sorbent, concentrating the hazardous pollutant, as well as valorizing the metal. Accordingly, U(VI) and Cd(II) desorption from the loaded commercial resin, C100H, were investigated using different concentrations of various acidic solutions. Briefly, 0.05 g of loaded resin is contacted with 10 mL of acidic aqueous solutions at room temperature for 24 h. The desorption results explored in Fig. 12 show that 1.0 M sulfuric acid

**Fig. 11** The relation between  $\text{Log } K_d$  and  $\text{Log}$  phosphoric acid molarity

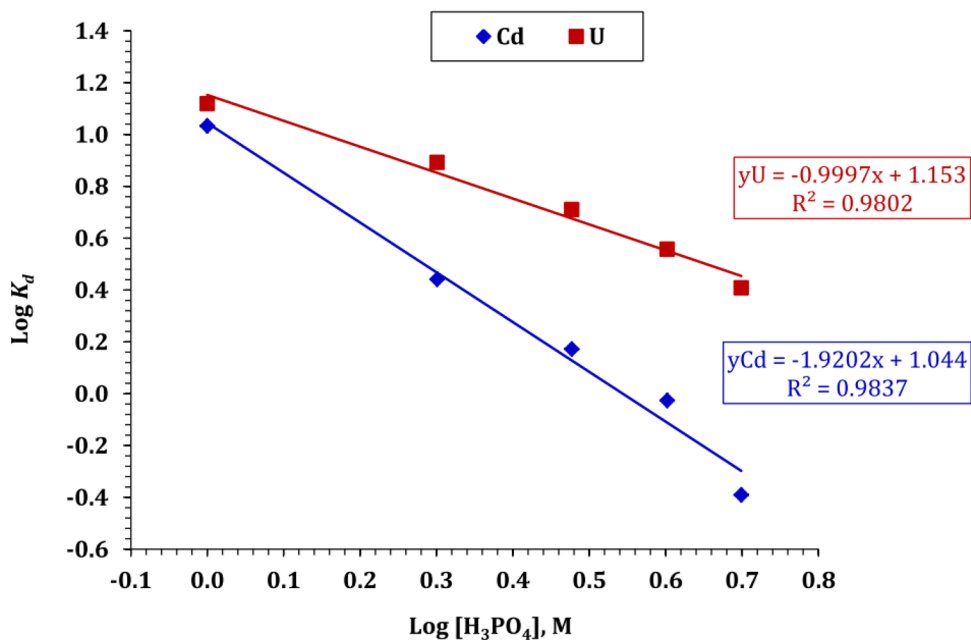


**Fig. 12** Cadmium and uranium desorption using different solutions

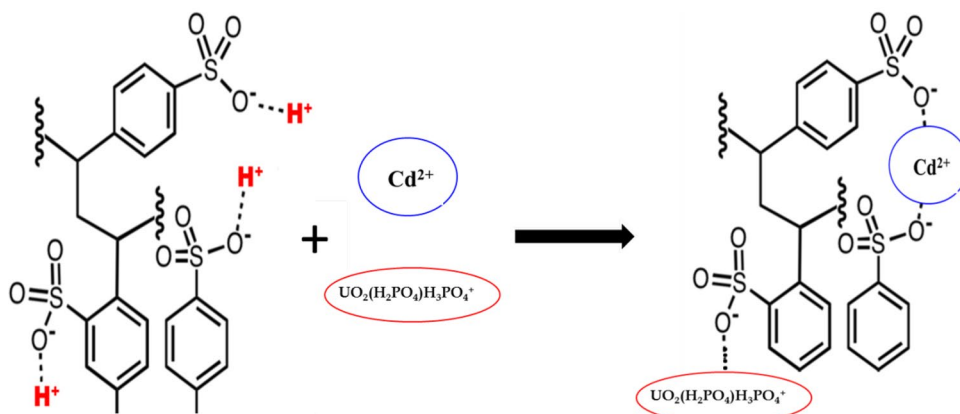
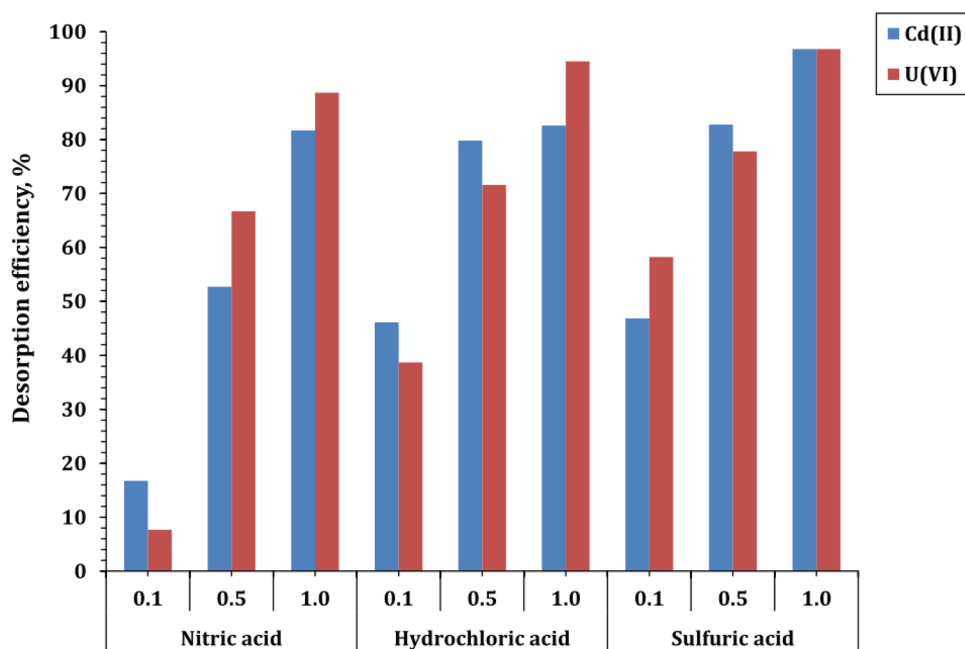


**Fig. 13** The proposed mechanism diagram of the adsorption of uranium and cadmium ions by functional groups on C100H resin



is suitable for eluting about 96% of U(VI) and Cd(II) ions from the loaded resin. The mechanism diagram of the adsorption of uranium and cadmium ions by functional groups on C100H resin could be proposed as displayed in Fig. 13.

### Recycling investigation

The performance of the commercial cation exchanger C100H resin for several cycles of uranium and cadmium sorption/desorption has been studied. The obtained data in Table 6 declare that the sorption and desorption efficiencies remain remarkably stable for the 5 cycles: around 93.5%, and 95.5% for Cd(II), and U(VI), respectively which reveals the feasibility of resin recycling.

**Table 6** Sorption/desorption cycles for Cd(II) and U(VI) ions removal using C100H resin

Cycle no	Cd(II) <i>E</i> (%)	U(VI) <i>E</i> (%)
1	95.4	96.8
2	94.3	96.1
3	93.6	95.6
4	92.9	94.8
5	92.1	94.1

### Conclusion

Uranium and cadmium ions recovery from crude dihydrate phosphoric acid has been performed using commercial cationic exchanger resin (C100H). The main parameters such as sorbent dose, reaction time and sorption temperature, as

well as the sorption kinetic and isotherm have been performed. The acquired data display that 60 min represents the sorption equilibrium for both metal ions. The commercial resin exhibit higher sorption tendency for U(VI) than Cd(II) ions, whereas the sorption capacity was about 14.6 and 3.3 mg/g for uranium and cadmium ions respectively. The sorption isotherm could be described successfully using Langmuir isotherm model. The sorption results are obeyed to the pseudo second order kinetic model. Uranium and cadmium desorption has been achieved using 1.0 M sulfuric acid. The resin recycling investigation displayed that the resin exhibit remarkable stability for five successive cycles of sorption/desorption.

## References

- Ye Y, Al-Khaleedi N, Barker L, Darwish MS, El Naggat AMA, El-Yahyaoui A, Hussein A, Hussein E-S, Shang D, Taha M, Zheng Y, Zhong J, Haneklaus N (2019) Uranium resources in China's phosphate rocks—identifying low-hanging fruits. *IOP Conf Ser Earth Environ Sci* 227:052033. <https://doi.org/10.1088/1755-1315/227/5/052033>
- Geissler B, Mew MC, Steiner G (2019) Phosphate supply security for importing countries: developments and the current situation. *Sci Total Environ* 677:511–523. <https://doi.org/10.1016/j.scitotenv.2019.04.356>
- Daneshgar S, Callegari A, Capodaglio A, Vaccari D (2018) The potential phosphorus crisis: resource conservation and possible escape technologies: a review. *Resources* 7(2):37. <https://doi.org/10.3390/resources7020037>
- Van Kernebeek HRJ, Oosting SJ, van Ittersum MK, Ripoll-Bosch R, de Boer IJM (2018) Closing the phosphorus cycle in a food system: insights from a modelling exercise. *Animal* 12(8):1755–1765. <https://doi.org/10.1017/S1751731118001039>
- Fayiga AO, Nwoke OC (2016) Phosphate rock: origin, importance, environmental impacts, and future roles. *Environ Rev* 24(4):403–415. <https://doi.org/10.1139/er-2016-0003>
- Geissler B, Mew MC, Weber O, Steiner G (2015) Efficiency performance of the world's leading corporations in phosphate rock mining. *Resour Conserv Recycl* 105:246–258. <https://doi.org/10.1016/j.resconrec.2015.10.008>
- Faridullah F, Umar M, Alam A et al (2017) Assessment of heavy metals concentration in phosphate rock deposits, Hazara basin, Lesser Himalaya Pakistan. *Geosci J* 21:743–752. <https://doi.org/10.1007/s12303-017-0013-9>
- Haneklaus N, Sun Y, Bol R, Lottemoser B, Schnug E (2017) To extract, or not to extract uranium from phosphate rock, that is the question. *J Environ Sci Technol* 51:753–754
- Mar SS, Okazaki M (2012) Investigation of Cd contents in several phosphate rocks used for the production of fertilizer. *Microchem J* 104:17–21. <https://doi.org/10.1016/j.microc.2012.03.020>
- Gaafar I, El-Shershaby A, Zeidan I, El-Ahli LS (2016) Natural radioactivity and radiation hazard assessment of phosphate mining, Quseir-Safaga area, Central Eastern Desert, Egypt. *NRIAG J Astron Geophys* 5(1):160–172. <https://doi.org/10.1016/j.nrjag.2016.02.002>
- Mousa MA, Gado HS, Abd-El Fattah MMG, Madi AE, Taha MH, Roshdy OE (2013) Removal of uranium from crude phosphoric acid by precipitation technique. *Arab J Nucl Sci Appl* 46(2013):38–47
- Kouzbour S, Gourich B, Gros F, Vial C, Allam F, Stiriba Y (2019) Comparative analysis of industrial processes for cadmium removal from phosphoric acid: a review. *Hydrometallurgy* 188:222–247
- Ahmed IM, Ammanoeil RN, Saad EA, Daoud JA (2019) Purification of crude phosphoric acid and leached apatite by solvent extraction with CYANEX 923 in kerosene. *Period Polytech Chem Eng* 63:122–129
- Ali HF, Ali MM, Taha MH, Abdel-Magied AF (2012) Uranium extraction mechanism from analytical grade phosphoric acid using D<sub>2</sub>EHPA and synergistic D<sub>2</sub>EHPA-TOPO mixture. *Int J Nucl Energy Sci Eng* 2:57–61
- Aly MM, Mousa MA, Taha MH, Kandil KM, El-Zoghby AA (2013) Kinetics and thermodynamics of uranium adsorption from commercial di-hydrate phosphoric acid using D<sub>2</sub>EHPA-impregnated charcoal. *Arab J Nucl Sci Appl* 46:29–37
- Singh DK, Mondal S, Chakravarty JK (2016) Recovery of uranium from phosphoric acid: a review. *Solvent Extr Ion Exch* 34(3):201–225
- Taha MH, Masoud AM, Khawassek YM, Hussein AEM, Aly HF, Guibal E (2020) Cadmium and iron removal from phosphoric acid using commercial resins for purification purpose. *Environ Sci Pollut Res*. <https://doi.org/10.1007/s11356-020-09342-7>
- Taha MH (2020) Solid-liquid extraction of uranium from industrial phosphoric acid using macroporous cation exchange resins: MTC1600H, MTS9500, and MTS9570. *Sep Sci Technol*. <https://doi.org/10.1080/01496395.2020.1787446>
- Hérès X, Blet V, Di Natale P, Ouattou A, Mazouz H, Dhiba D, Cuer F (2018) Selective extraction of rare earth elements from phosphoric acid by ion exchange resins. *Metals* 8(9):682
- Nagaphani Kumar B, Radhika S, Ramachandra Reddy B (2010) Solid-liquid extraction of heavy rare-earths from phosphoric acid solutions using Tulsion CH-96 and T-PAR resins. *Chem Eng J* 160(1):138–144
- Outokesh M, Tayyebi A, Khanchi A, Grayeli F, Bagheri G (2011) Synthesis and characterization of new biopolymeric microcapsules containing DEHPA-TOPO extractants for separation of uranium from phosphoric acid solutions. *J Microencapsul* 28:248–257
- El-Bayaa AA, Badawy NA, Gamal AM, Zidan IH, Mowafy AR (2011) Purification of wet process phosphoric acid by decreasing iron and uranium using white silica sand. *J Hazard Mater* 190(1–3):324–329. <https://doi.org/10.1016/j.jhazmat.2011.03.037>
- Taha MH, El-Maadawy MM, Hussein AM, Youssef W (2018) Uranium sorption from commercial phosphoric acid using kaolinite and metakaolinite. *J Radioanal Nucl Chem* 317:685–699
- Singh DK, Yadav KK, Varshney L, Singh H (2013) Recovery of uranium from phosphoric acid medium by polymeric composite beads encapsulating organophosphorus extractants. *GLOBAL-2013: International nuclear fuel cycle conference, September 29–October 3 2013, Salt Lake City, UT, pp 44–52*
- El-Sofany EA, Zaher WF, Aly HF (2009) Sorption potential of impregnated charcoal for removal of heavy metals from phosphoric acid. *J Hazard Mater* 165(1–3):623–629. <https://doi.org/10.1016/j.jhazmat.2008.10.037>
- Taha MH (2021) Sorption of U(VI), Mn (II), Cu(II), Zn(II), and Cd(II) from multi-component phosphoric acid solutions using MARATHON C resin. *Environ Sci Pollut Res Int* 28(10):12475–12489. <https://doi.org/10.1007/s11356-020-11256-3> (**Epub 2020 Oct 20 PMID: 33079349**)
- Cheira MF (2015) Characteristics of uranium recovery from phosphoric acid by an aminophosphonic resin and application to wet process phosphoric acid. *Eur J Chem* 6(1):48–56
- Marzenko Z, Balcerzak M (2000) Uranium. In: Marzenko Z, Balcerzak M (eds) *Separation, preconcentration and spectrophotometry in inorganic analysis*, vol 10. Elsevier, Amsterdam, pp 446–455

29. Farag NM, El-sayed GO, Morsy AMA, Taha MH, Yousif MM (2015) Modification of Davies & Gray method for uranium determination in phosphoric acid solutions. *Int J Adv Res.* 3:323–337
30. Hussein AEM, Taha MH (2013) Uranium removal from nitric acid raffinate solution by solvent immobilized PVC cement. *J Radioanal Nucl Chem* 295(1):709–715
31. Massoud A, Masoud AM, Youssef WM (2019) Sorption characteristics of uranium from sulfate leach liquor by commercial strong base anion exchange resins. *J Radioanal Nucl Chem.* <https://doi.org/10.1007/s10967-019-06770-9>
32. Largitte L, Pasquier R (2016) A review of the kinetics adsorption models and their application to the adsorption of lead by an activated carbon. *Chem Eng Res Des* 109:495–504. <https://doi.org/10.1016/j.cherd.2016.02.006>
33. Masoud AM (2020) Sorption behavior of uranium from sulfate media using purolite A400 as a strong base anion exchange resin. *Int J Environ Anal Chem.* <https://doi.org/10.1080/03067319.2020.1763974>
34. Rajak VK, Kumar S, Thombre NV, Mandal A (2018) Synthesis of activated charcoal from saw-dust and characterization for adsorptive separation of oil from oil-in-water emulsion. *Chem Eng Commun* 205(7):897–913
35. Khawassek YM, Masoud AM, Taha MH, Hussein AEM (2018) Kinetics and thermodynamics of uranium ion adsorption from waste solution using Amberjet 1200 H as cation exchanger. *J Radioanal Nucl Chem* 315(3):493–502. <https://doi.org/10.1007/s11356-020-09342-7>
36. Foo KY, Hameed BH (2010) Insights into the modeling of adsorption isotherm systems. *Chem Eng J* 156(1):2–10
37. Cheira MF, Zidan IH, Manaa EA (2014) Potentiality of white sand for the purification of wet process phosphoric acid from some metallic elements (U, Zn, Cd). *Chem Technol Indian J* 9(6):224–233
38. Hinojosa Reyes L, Saucedo Medina I, Navarro Mendoza R, Revilla Vázquez J, Avila Rodríguez M, Guibal E (2001) Extraction of cadmium from phosphoric acid using resins impregnated with organophosphorus extractants. *Ind Eng Chem Res* 40(5):1422–1433. <https://doi.org/10.1021/ie0005349>
39. Zhang R, Chen C, Li J, Wang X (2015) Preparation of montmorillonite @ carbon composite and its application for U(VI) removal from aqueous solution. *Appl Surf Sci* 349:129–137
40. Taha MH, Abdel Maksoud SA, Ali MM, El Nagggar AMA, Morshey AS, Elzoghby AA (2019) Conversion of biomass residual to acid-modified bio-chars for efficient adsorption of organic pollutants from industrial phosphoric acid: an experimental, kinetic and thermodynamic study. *Int J Environ Anal Chem* 99:1211–1234
41. Wu F-C, Tseng R-L, Juang R-S (2009) Initial behavior of intraparticle diffusion model used in the description of adsorption kinetics. *Chem Eng J* 153:1–8
42. Malash GF, El-Khaiary MI (2010) Piecewise linear regression: a statistical method for the analysis of experimental adsorption data by the intraparticle-diffusion models. *Chem Eng J* 163:256–263
43. Canner AJ, Pepper SE, Hayer M, Ogden MD (2018) Removal of radionuclides from a HCl steel decontamination stream using chelating ion exchange resins—initial studies. *Prog Nucl Energy* 104:271–279. <https://doi.org/10.1016/j.pnucene.2017.10.007>
44. Morsy AMA, Hussein AEM (2012) Retention of uranium from liquid waste solution onto Egyptian natural clay. *Isotope Radiat Res* 44:537–550

**Publisher's Note** Springer Nature remains neutral with regard to jurisdictional claims in published maps and institutional affiliations.